Potential role of poly (ADP-ribose) polymerase in delayed cerebral vasospasm following subarachnoid hemorrhage in rats

YAMENG FAN[1*], GE YAN[2*], FURONG LIU[1], JIE RONG[1], WENXIA MA[1], DANRONG YANG[1] and YAN YU[1]

[1]Department of Public Health, Medical College of Xi'an Jiaotong University; [2]Department of Medical Image, The First Affiliated Hospital of Xi'an Jiaotong University, Xi'an, Shaanxi 710061, P.R. China

Received April 6, 2018; Accepted November 14, 2018

DOI: 10.3892/etm.2018.7073

Abstract. Poly (ADP-ribose) polymerase (PARP) serves a key role in several neurological disorders, however, the specific role of PARP in delayed cerebral vasospasm (DCVS) following subarachnoid hemorrhage (SAH) remains unclear. The present study was conducted to clarify the possible mechanism of PARP in DCVS with the treatment of 3-aminobenzamide (3-AB), a PARP inhibitor. In the preliminary experiment, an internal carotid artery puncture SAH model, a cisterna magna double injection SAH model and prechiasmatic cistern single injection SAH model were compared with respect to mortality and neurobehavioral test results. The prechiasmatic cistern single injection SAH model was chosen to induce DCVS in the formal experiment. In the formal experiment, a total of 96 Sprague Dawley rats were randomly allocated into the sham group, the SAH group and the SAH+3-AB group and then each group was further subdivided into days 3, 5, 7 and 14 post-SAH subgroups (n=8 for each subgroup). The prechiasmatic cistern single injection SAH model was established to induce DCVS. Neurobehavioral testing and HE staining were conducted to evaluate the degree of cerebral vasospasm. PARP activity was assessed by ELISA and immunohistochemistry. An electrophoretic mobility shift assay was used to detect nuclear factor (NF)-κB DNA-binding activity. The expression of monocyte chemotactic protein 1 (MCP-1) and C-reactive protein (CRP) were measured by western blotting. Cerebral vasospasm occurred following SAH and became most severe on around day 7 post-SAH. NF-κB activity, PARP activity, the expression of MCP-1 and CRP exhibited a similar time course to cerebral vasospasm. Treatment with 3-AB alleviated the degree of cerebral vasospasm. NF-κB activity, PARP activity and the expression of MCP-1 and CRP were also suppressed by 3-AB treatment. In conclusion, PARP may serve an important role in regulating the inflammatory response and ultimately contribute to DCVS. Therefore 3-AB may be a potential therapeutic agent for DCVS.

Correspondence to: Professor Yan Yu, Department of Public Health, Medical College of Xi'an Jiaotong University, 76 West Yanta Road, Xi'an, Shaanxi 710061, P.R. China
E-mail: yuyan@mail.xjtu.edu.cn

*Contributed equally

Abbreviations: PARP, poly ADP-ribose polymerase; DCVS, delayed cerebral vasospasm; 3-AB, 3-aminobenzamide; NF-κB, nuclear factor-κB; MCP-1, monocyte chemotactic protein-1; CRP, C-reactive protein; 3AB, 3-aminobenzamide; TNF-α, tumor necrosis factor-α; ICAM-1, intercellular adhesion molecule-1; NAD, nicotinamide adenine dinucleotide; I-κB, inhibitor-κB; CVS, cerebral vasospasm; TBST, tris buffered saline tween

Key words: delayed cerebral vasospasm, subarachnoid hemorrhage, inflammatory response, poly ADP-ribose polymerase, nuclear factor-κB, 3-AB

Introduction

About five percent of stroke is caused by subarachnoid hemorrhage (SAH) (1). The most common complications of SAH are cerebral edema, rehaemorrhagia, delayed cerebral ischemia and delayed cerebral vasospasm (DCVS), among which DCVS is the most serious and potentially fatal complication for SAH patients (2).

In the present study of SAH, there are three most popular models: Internal carotid artery puncture SAH model, cisterna magna double injection SAH model and prechiasmatic cistern single injection SAH model. An ideal SAH model for DCVS study should accurately follow the time course of vasospasm in humans at a low mortality rate. But controversy still exists regarding which was the most appropriate method for DCVS study (3). Therefore, a preliminary experiment was conducted to compare these three models (Fig. 1).

Accumulating evidence suggested that the inflammatory response is crucial in the development of DCVS. Several morphological studies (4-6) have demonstrated that there are a large number of inflammatory cells infiltrating the spastic vessel wall and its surrounding tissues in the development of DCVS. The study by Handa *et al* (7) has also indicated that the elevated expression of intercellular adhesion molecule-1 (ICAM-1) may contribute to the development of DCVS. In addition, a number of other inflammatory cytokines, including interleukin (IL)-1β, IL-6 and tumor necrosis factor (TNF)-α have been demonstrated to be increased in the DCVS following SAH (8,9). All the above-mentioned increased inflammatory

factors are associated with DCVS, so it's reasonable to assume that the inflammatory response may be involved in DCVS following SAH.

Poly (ADP-ribose) polymerase (PARP), a kind of post-translational modification enzyme, exists widely in eukaryote cells except yeasts, serving a key role in DNA damage identification and DNA repair (10). When DNA damage appears, PARP could subsequently recognize and bind to DNA breakage, then be activated. The activated PARP causes further depletion of nicotinamide adenine dinucleotide (NAD^+) and the formation of poly (ADP-ribose) chain, which finally lead to DNA repair (11). Beyond that, it has been reported that PARP could mediate inflammation-associated gene expression through interactions with transcription factors, particularly, nuclear factor (NF)-κB (12). NF-κB, a nuclear transcription regulatory factor stays inactive in the cytoplasm bound to the inhibitor-κB (I-κB) protein in the resting state but translocates to the nucleus following degradation of I-κB once activated (13). The translocated NF-κB could bind specifically to the κB sequence in the chromatin and subsequently initiate genes transcription associated with inflammation, including cytokines, adhesion molecules, and chemokines (9).

This study was conducted to investigate the potential role of PARP in the development of DCVS following SAH. Furthermore, as a competitive inhibitor of PARP, the effect of 3-aminobenzamide (3-AB) on DCVS was also investigated.

Materials and methods

Animals. A total of 216 adult male Sprague-Dawley (SD) rats (180±20 g) were purchased from the Animal Center of Xi'an Jiaotong University (Xi'an, China). Ethical approval was obtained from the Ethical Committee of Xi'an Jiaotong University. The rats were raised in a 12-h light/dark cycle under a required temperature (25±2˚C) and humidity (50±10%) with free access to feed and water.

Rat SAH model. The prechiasmatic cistern single injection SAH model was used in the formal experiment. Following anesthesia with 2% isoflurane in oxygen, the rat was placed first in dorsal recumbency. Aided by a surgical microscope, a small inguinal incision was made to access the femoral artery to take blood. Then the rat was placed in ventral recumbency. With the head fixed on the stereotactic instrument (51600; Stoelting, Co., Wood Dale, IL, USA), the surgical site in the calvarium was shaved and disinfected prior to the sagittal incision, exposing the surface of skull. After drilling a hole 7.5 mm anterior to the bregma in the midline, the fresh autologous nonheparinized blood (0.3 ml) from the femoral artery was slowly injected into the prechiasmatic cistern in 20 sec by a self-made catheter in the SAH group. In the sham group, the rat was injected equivalent artificial cerebrospinal fluid (0.3 ml) instead of the blood from femoral artery. At the end of surgery, the hole was sealed with the dental cement and the incision was sutured. The rat was placed in a head-down prone position for ~30 min and returned to the cage. In addition, internal carotid artery puncture SAH model and cisterna magna double injection SAH model were also used in the preliminary experiment as previously described (3). Briefly, the internal carotid artery puncture SAH model was established by puncturing a 3-0 nylon filament into the internal carotid artery and the cisterna magna double injection SAH model was achieved by repeating a second injection 48 h following injecting the fresh autologous blood (0.3 ml) into the cisterna magna.

Experimental design. In the preliminary experiment, a total of 120 rats were randomly assigned to three group: Internal carotid artery puncture SAH model group (n=40), the cisterna magna double injection SAH model group (n=40) and the prechiasmatic cistern single injection SAH model group (n=40). In the formal experiment, a total of 96 SD rats were randomly assigned to three groups: The sham group (n=32), SAH group (n=32) and SAH+3-AB group (n=32), and then each group was further subdivided into days 3, 5, 7 and 14 post-SAH subgroups (n=8 for each subgroup). As mentioned, the rats in the sham group were injected with artificial cerebrospinal fluid (0.3 ml), while the rats in the SAH group were injected with autologous nonheparinized blood (0.3 ml) from the femoral artery. Following injection with autologous nonheparinized blood (0.3 ml), the rats in SAH+3-AB group were injected with 3-AB (30 mg/kg) via femoral vein on days 0 and 1, while the rats in the SAH group were treated with equivalent saline (0.9% NaCl) as controls.

Assessment of neurobehavioral score. The neurobehavioral score was evaluated prior to euthanasia according to the grading system proposed by Kaoutzanis *et al* (14), which could efficiently estimate motor ability, eye response and eating habit of rats. Grading was performed in different groups. The rating criteria are presented in Table I.

HE staining. The rats were sacrificed on days 3, 5, 7, 14 post-SAH according to the subgroups. The rat brains were surgically collected for further experiments. The isolated basilar artery was embedded by tissue embedding station (KD-BMII; Kedee Pathology Instruments, Co., Ltd., Zhejiang, China) and made into paraffin sections by microtome (RM2235; Leica Microsystems GmbH, Wetzlar, Germany). According to a previous study (15), brainstems were fixed with 10% formalin for 24 h at 4˚C and the paraffin-embedded basilar artery sections (4-μm in thickness) were deparaffinized, hydrated, washed, and stained with hematoxylin and eosin at room temperature for 10 and 5 min, respectively. By observing the pathology of basilar artery under a light microscope (BX40; Olympus Corporation, Tokyo, Japan), the wall thickness and internal diameter were calculated using an image analysis system (Q550CW; Leica Microsystems GmbH).

Immunohistochemical study. Following the protocol of the Histostain-SP kit (OriGene Technologies, Inc., Rockville, MD, USA) and DAB substrate kit (OriGene Technologies, Inc.), the basilar artery sections were incubated with rabbit anti-poly (ADP-ribose) antibodies (1:500; cat. no. 4336-BPC-100; Trevigen, Gaithersburg, MD, USA) at 4˚C overnight. Sections were then incubated with horseradish peroxidase conjugated goat anti-rabbit IgG secondary antibodies (1:100; cat. no. SPN-9001; OriGene Technologies, Inc.) at 37˚C for 10 min, peroxidase anti-peroxidase complex (1:100; OriGene Technologies, Inc.) at 37˚C for 10 min and DAB (1:20) at room

Table I. Neurobehavioral score.

Neurobehavioral	Score
Motor ability	
Walk freely	5
Walk with difficultly	4
Unable to walk	3
Body contraction with stabbing pain	2
No response with stabbing pain	1
Eye response	
Open eyes by oneself	4
Open eyes with sound stimulation	3
Open eyes with stabbing pain	2
Be unable to open eyes	1
Eating habit	
Eat freely	2
Refuse to eat	1

The range of rating ranges from 3 (worst) to 11 (normal).

temperature for 5 min. PBS was used as a washing agent. The negative control used PBS instead of the primary antibody. The immunoreactive marks of poly (ADP-ribose) were observed under a light microscope (BX40; Olympus Corporation) and the average optical density was measured by an image analysis system (Q550CW; Leica Microsystems GmbH).

ELISA. The brain tissue was washed with PBS and cut into pieces. The pieces were placed into the tissue grinder and 1 ml PBS was added to make the homogenate, overnight at -20˚C. After repeated freezing and thawing for 2 times, the tissue homogenate was centrifuged at 5,000 x g at 4˚C for 5 min. Finally, the supernatant was sub-packed and stored at -80˚C. According to manufacturer's protocol of the Rat-PARP ELISA assay kit (cat. no. LS-F33291-1; LifeSpan BioSciences Inc., Seattle, Washington, USA), the standards and samples were incubated in the pre-coated 96-well plate at 37˚C for 30 min. PARP antibodies were then incubated in the plates at 37˚C for 30 min. Finally, the chromogenic substrate was added to the plate. The PARP level was quantified using a microplate reader (1510; Thermo Fisher Scientific, Inc.).

Electrophoretic mobility shift assay (EMSA). NF-κB consensus oligos are 5'-AGTTGAGGGGACTTTCCCAGGC-3' and 3'-TCAACTCCCCTGAAAGGGTCCG-5', which were end-labeled with biotin (cat. no. E3291; Promega Corporation, Madison, WI, USA). Nuclear extracts (5 μg) were preincubated in a binding buffer for 20 min at room temperature. The activity of NF-κB was analyzed using a commercial EMSA assay kit (cat. no. E3050; Promega Corporation) following the manufacturer's protocol. The DNA-protein complexes were resolved from the free DNA probe on a 4% non-denaturing polyacrylamide gel by electrophoresis. The gels were subsequently transferred to nylon membranes and subjected to the autoradiography. Finally, an image analysis system (Q550CW; Leica Microsystems GmbH) was used to analyze the NF-κB activity.

Western blot analysis. Western blotting was performed as previously reported (16). Brain tissue was lysed using the radioimmunoprecipitation lysis buffer kit (Xi'an Hat Biotechnology Co., Ltd., Xi'an, China). Total protein was determined using a bicinchoninic assay kit (Beyotime Institute of Biotechnology, Haimen, China). Equal quantities (25 μg) of protein were resolved by 10% SDS-PAGE with electrophoresis apparatus (DYCZ-40B; Beijing Liuyi Biotechnology Co., Ltd., Beijing, China) and further transferred onto polyvinylidene difluoride membranes, which were soaked with methanol for 30 sec. After blocking with 5% nonfat milk for 1 h at room temperature, samples were probed with MCP-1 (1:1,000; cat. no. 2027S; Cell Signaling Technology Inc., Danvers, MA, USA), CRP (1:1,000; cat. no. 14316S; Cell Signaling Technology Inc.) and GAPDH antibodies (1:1,000; cat. no. 5174T; each, Cell Signaling Technology Inc.) at 4˚C overnight, the membrane was washed three times with tris buffered saline tween (TBST; 1xTBS with 0.1% Tween-20) and incubated with horseradish peroxidase (HRP) conjugated goat anti-rabbit IgG (1:5,000; cat. no. ab205718, Abcam, Cambridge, UK) at room temperature for 1 h. Finally, the protein bands were visualized using the Immobilon Western Chemiluminescent HRP Substrate kit (EMD Millipore, Billerica, MA, USA) and quantified by an image analysis system (Q550CW; Leica Microsystems GmbH).

Statistical analysis. Each experiment was conducted at least three times. SPSS18.0 statistical software (SPSS, Inc., Chicago, IL, USA) was used for data analysis. All quantitative data were represented as the mean ± standard deviation. Comparisons among multiple groups were performed by one-way analysis of variance followed by Tukey's test used for post hoc comparison. Fisher's exact test was used for successful rate of inducing DCVS analysis. $P<0.05$ was considered to indicate a statistically significant difference.

Results

Comparison of three SAH models in the preliminary experiment. The percentage mortality in the internal carotid artery puncture SAH model group, cisterna magna double injection SAH model group and prechiasmatic cistern single injection SAH model group was 67.5% (27 of 40 rats), 42.5% (17 of 40 rats) and 22.5% (9 of 40 rats) respectively ($P<0.05$; Fig. 1A). The internal carotid artery puncture model was excluded first for displaying an unacceptably high percentage mortality.

According to the assessment of neurobehavioral score, the neurobehavioral impairment occurred in most rats from the remaining two groups (cisterna magna double injection SAH model group and prechiasmatic cistern single injection SAH model group) on days 3 to 5 post-SAH and reached the most serious level on around day 7 post-SAH, and returned to normal on about 2 weeks post-SAH (Fig. 1B). There were 16 of the surviving rats (16 of 23, 69.6%) in the cisterna magna double injection SAH model group and 23 of the surviving rats (23 of 31, 74.2%) in the prechiasmatic cistern single injection SAH model group that were suffering from the above phenomena, indicating the occurrence of DCVS and the formation of a successful model (Fig. 1C).

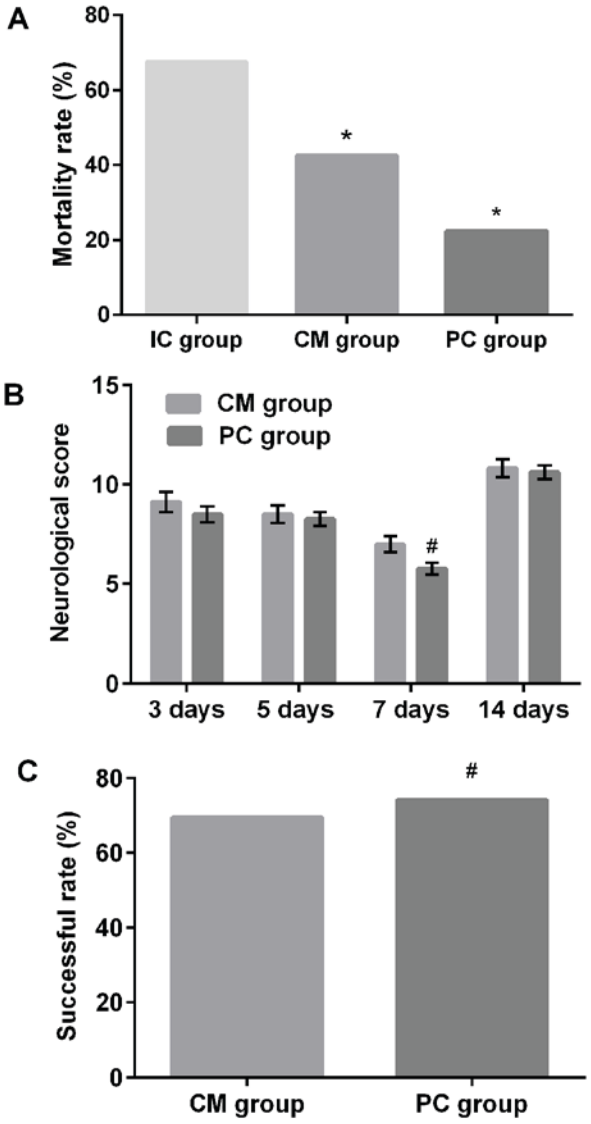

Figure 1. The mortality, time course of neurological deficit score following SAH and the successful rate of inducing DCVS in different model group. (A) Mortality was calculated in the three groups and (B) neurological deficit scores were evaluated on days 3, 5, 7, 14 post-SAH. The successful rate of inducing DCVS was then calculated (C). The success rate of model formation was calculated by the proportion of rats, which were suffering typical characteristic of DCVS according to the neurobehavioral score. The IC group, the CM group and the PC group were compared. *P<0.05 vs. IC group; #P<0.05 vs. CM group. SAH, subarachnoid hemorrhage; DCVS, delayed cerebral vasospasm; IC, internal carotid artery puncture SAH model; CM, cisterna magna double injection SAH model; PC, prechiasmatic cistern single injection SAH model group.

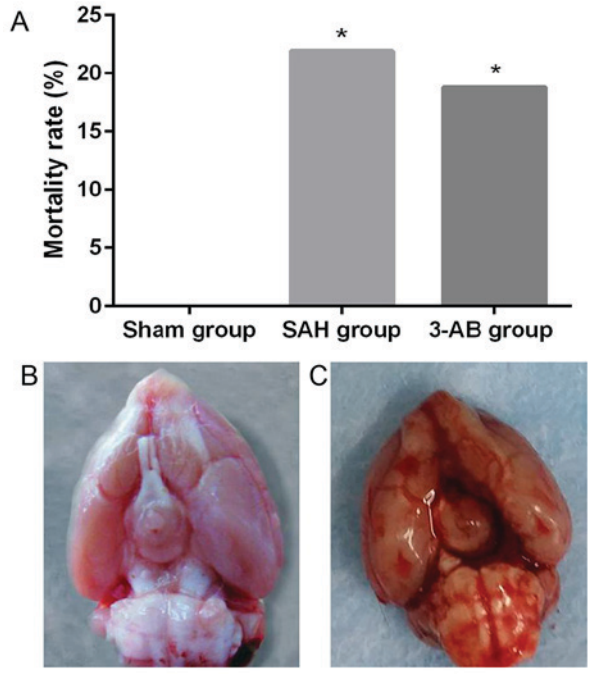

Figure 2. Mortality and macroscopic observation of rat brain following SAH. (A) The mortality was calculated in each group. (B) No obvious blood clots were observed in sham group. (C) A large amount of blood clots were observed surrounding the arteries in SAH group. SAH, subarachnoid hemorrhage; 3-AB, 3-aminobenzamide. *P<0.05 vs. the sham group

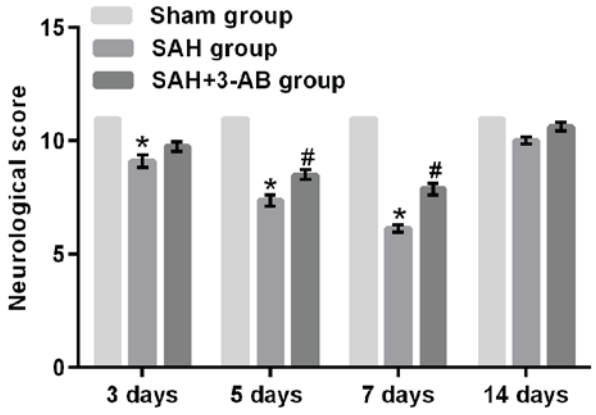

Figure 3. The time course of neurological deficit score following SAH and the effect of 3-AB on score. The neurological deficit scores were evaluated on days 3, 5, 7, 14 post-SAH in the sham group, SAH group and SAH+3-AB group. *P<0.05 vs. the sham group, #P<0.05 vs. the SAH group. SAH, subarachnoid hemorrhage; 3-AB, 3-aminobenzamide.

Mortality and general observation. There are three groups in the formal experiment: The sham group, SAH group and SAH+3-AB group. No mortality was observed in the sham group (0 of 32 rats). The percentage mortality in SAH group and SAH+3-AB group was 21.9% (7 of 32 rats) and 18.8% (6 of 32 rats) respectively (P<0.05; Fig. 2A). Blood clots were observed around the basilar artery in the SAH group, whereas no obvious blood clots were observed in the sham group (Fig. 2B and C).

Neurobehavioral deficit score. In the SAH group, the scores gradually decreased, reaching the lowest point on day 7 post-SAH and returned to normal on ~day 14 post-SAH (Fig. 3). Compared with the sham group, the rats in the SAH group expressed significantly different degrees of neurobehavioral impairment on days 3, 5 and 7 (P<0.05; Fig. 3). However, this effect was significantly alleviated by 3-AB treatment on days 5 and 7 (P<0.05; Fig. 3).

Morphological changes of the basilar artery. As detected by hematoxylin-eosin staining, the basilar artery in the sham group displayed a clear structure without wall thickening, luminal stenosis and contraction of the internal elastic lamina (Fig. 4A). In contrast, an obviously thickened vessel wall, narrowed

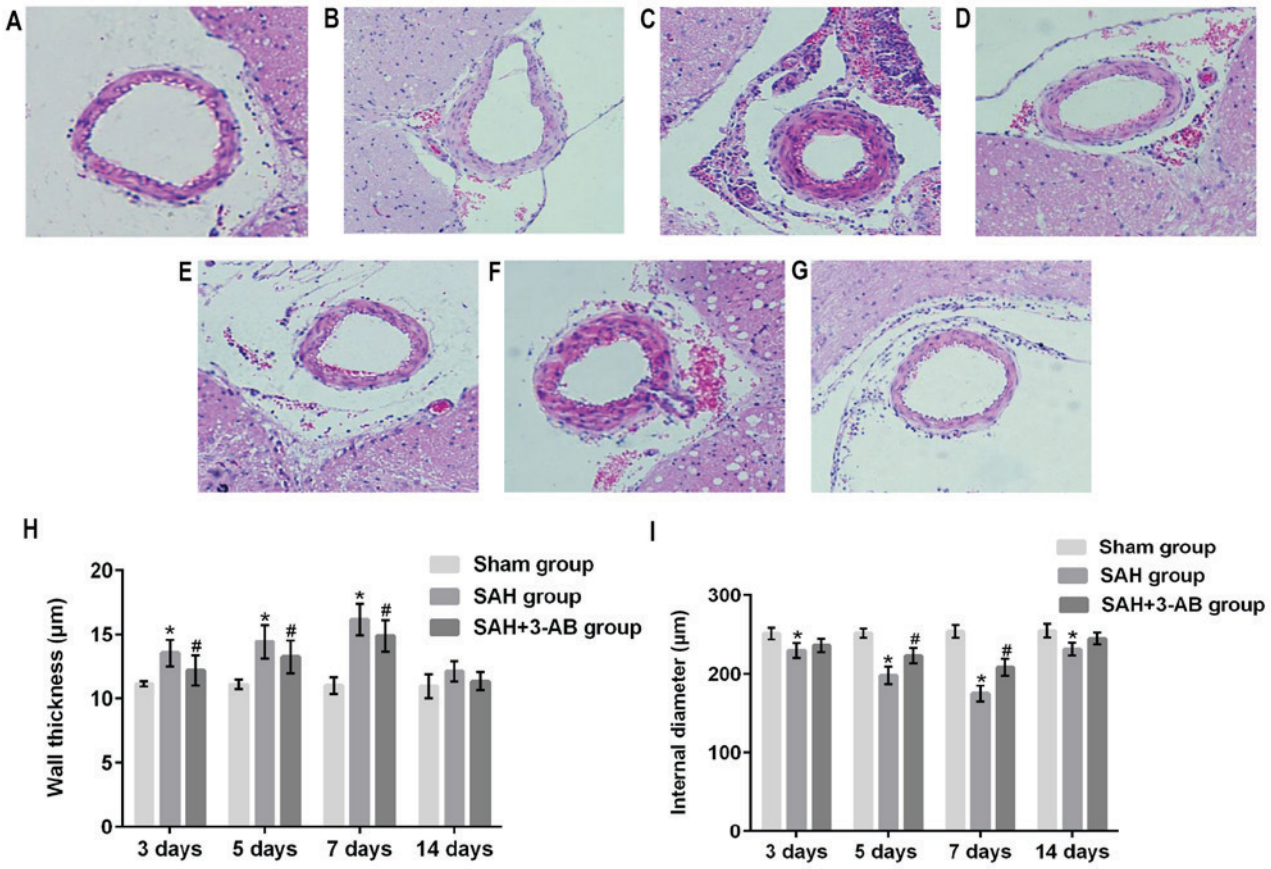

Figure 4. Representative morphological changes of basilar artery. The morphological changes were observed in (A) sham group, (B) SAH group on day 3, (C) SAH group on day 7, (D) SAH group on day 14, (E) SAH+3-AB group on day 3, (F) SAH+3-AB group on day 7, (G) SAH+3-AB group on day 14. The bar chart demonstrated the (H) wall thickness and (I) the internal diameter of the basilar artery in different groups. *P<0.05 vs. the sham group, #P<0.05 vs. the SAH group. SAH, subarachnoid hemorrhage; 3-AB, 3-aminobenzamide.

lumen, swelling endothelial cells and shrunken internal elastic lamina were observed in the SAH group (Fig. 4B-D). After SAH, all the above-mentioned pathological alterations became gradually more serious at first, then significant on day 7 and finally being alleviated by ~day 14 (Fig. 4B-D). Compared with the SAH group, the corrugation of the internal elastic lamina was alleviated, the wall thickness decreased and the luminal stenosis was relieved in the SAH+3-AB group (Fig. 4E-G).

Next, the wall thickness and the internal diameter of the basilar artery were measured at various time points in the different groups. The wall thickness increased initially, reaching the maximum thickness around day 7 then finally returning towards normal on day 14 (Fig. 4H). Similarly, the internal diameter of the artery narrowed first, reaching the most narrow point on ~day 7 and finally returned towards a normal diameter on day 14 (Fig. 4I). Compared with the sham group, the wall thickness in the SAH group was significantly increased on days 3, 5, 7 post-SAH (P<0.05; Fig. 4H) and this increase was significantly reversed following 3-AB treatment (P<0.05; Fig. 4H). Conversely, the internal diameter of the basilar artery in the SAH group was significantly decreased (P<0.05; Fig. 4I) and this decrease was significantly reversed following 3-AB treatment on days 5 and 7 post-SAH (P<0.05; Fig. 4I).

Immunohistochemistry of poly (ADP-ribose). In the sham group, the immunohistochemical staining of poly (ADP-ribose) was weak and sporadic (Fig. 5A). In the SAH group, the staining of poly (ADP-ribose) gradually increased over time, peaking on around day 7 and then reduced on day 14. In addition, compared with the sham group, the staining of poly (ADP-ribose) in the SAH group was observed across all layers of basilar artery, especially in endothelial cells (P<0.05; Fig. 5B-D). The staining of poly (ADP-ribose) in SAH+3AB group was lighter compared with the SAH group on days 3, 5 and 7 (P<0.05; Fig. 5E-G). The quantitative comparison is also presented (Fig. 5H).

ELISA of PARP. ELISA was also used to quantitatively analyze PARP activity. Similarly, PARP was gradually increased first following SAH, peaked on day 7 and then decreased on ~day 14 (Fig. 6). In the SAH group, PARP was significantly increased compared with the sham group at all time points (P<0.05; Fig. 6). 3-AB treatment significantly weakened this increase compared with SAH group on day 7 (P<0.05; Fig. 6).

Western blot of MCP-1 and CRP. Western blotting was used to detect the expression of MCP-1 and CRP. MCP-1 expression and CRP expression were increased following SAH at first, reaching the highest level on ~day 7 and finally decreasing (Fig. 7A and B). Compared with the sham group, the expression of MCP-1 and CRP in the SAH group were significantly

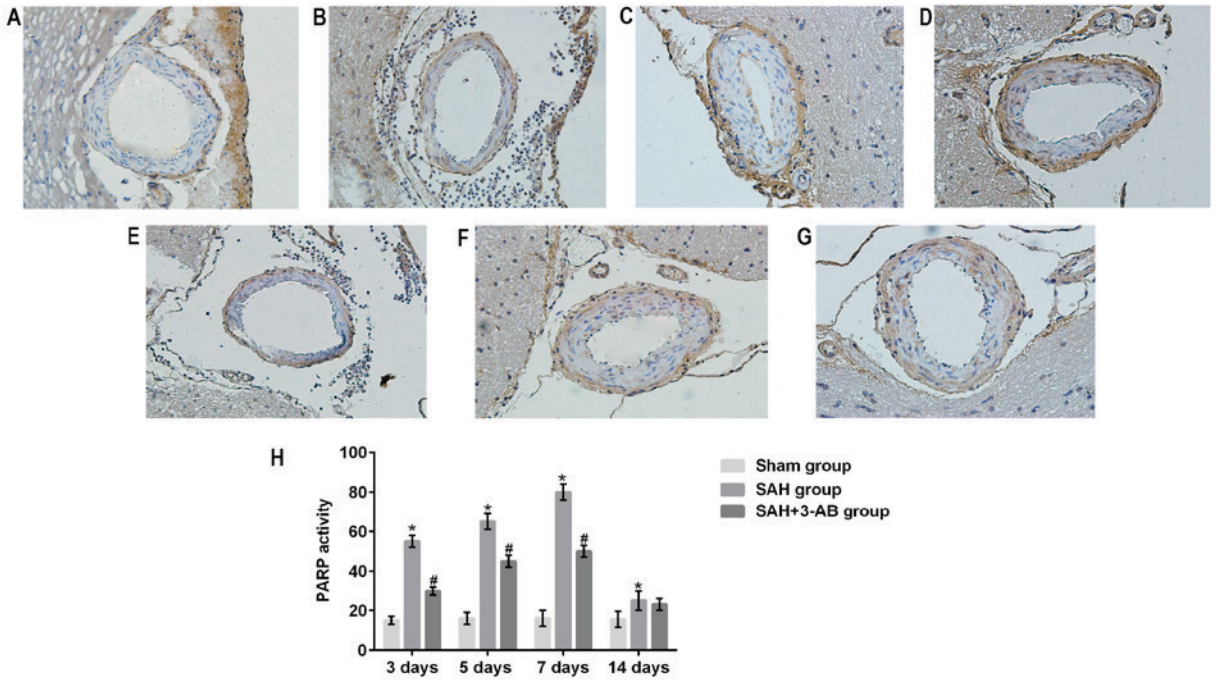

Figure 5. Representative immunohistochemical staining of poly (ADP-ribose) on basilar artery. The immunohistochemical staining was presented in (A) the sham group, (B) SAH group on day 3, (C) SAH group on day 7, (D) SAH group on day 14, (E) SAH+3-AB group on day 3, (F) SAH+3-AB group on day 7, (G) SAH+3-AB group on day 14. The brown products demonstrated positive results of poly (ADP-ribose). (H) The bar chart demonstrated the poly (ADP-ribose) level in different groups. *P<0.05 vs. the sham group, #P<0.05 vs. the SAH group. SAH, subarachnoid hemorrhage; 3-AB, 3-aminobenzamide.

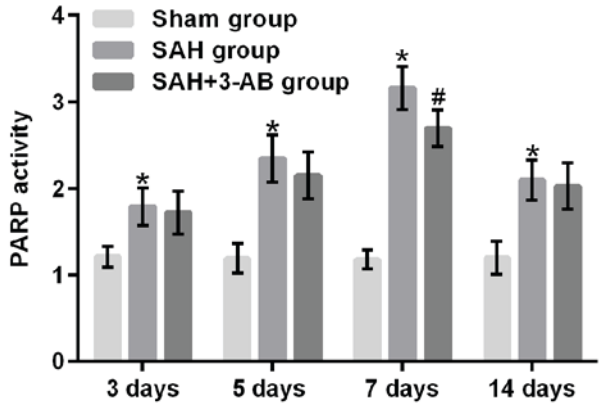

Figure 6. The time course of PARP activity following SAH and the effect of 3-AB on PARP. PARP activity was detected by ELISA on days 3, 5, 7, 14 post-SAH in sham group, SAH group and SAH+3-AB group. *P<0.05 vs. the sham group, #P<0.05 vs. the SAH group. SAH, subarachnoid hemorrhage; 3-AB, 3-aminobenzamide.

increased (P<0.05; Fig. 7). In the SAH+3-AB group, the expression of MCP-1 and CRP exhibited a significant reduction on days 3, 5 and 7 post-SAH compared with the SAH group (P<0.05; Fig. 7).

EMSA of NF-κB. EMSA was used to analyze NF-κB DNA-binding activity. NF-κB DNA-binding activity was increased following SAH at first, reached the highest level on around day 7 and then declined (Fig. 8). NF-κB DNA-binding activity in SAH group was significantly increased compared with the sham group (P<0.05), while significantly reduced following 3-AB treatment (P<0.05).

Discussion

According to clinical presentation and experimental data (15,17,18), cerebral vasospasm (CVS) can be divided into two types, acute CVS and DCVS. Acute CVS arises immediately following SAH and recovers within several hours. Unlike the clinical course of acute CVS, DCVS typically occurs on days 3-5 post-SAH, peaks o-n around day 7 following SAH and is improves by ~2 weeks post-SAH.

Since DCVS is a major cause of mortality and disability in patients surviving SAH, it is crucial to establish a good DCVS post-SAH model for studying the pathogenesis of DCVS further. However, the most appropriate model for DCVS study is still controversial (19). A total of three of the most common SAH models, internal carotid artery puncture SAH model, cisterna magna double injection SAH model and prechiasmatic cistern single injection SAH model, were compared in the preliminary experiment to induce DCVS. The internal carotid artery puncture model was excluded first for displaying an unacceptable mortality rate in the first 24 h. Compared with the cisterna magna double injection model, the prechiasmatic cistern single injection model could better induce DCVS with the relatively low percentage mortality of 22.5%. Therefore, the prechiasmatic cistern single injection SAH model was chosen for use in the latter experiment.

Neurobehavioral tests and HE staining were performed to assess the different aspects of DCVS degree in the formal study. Generally, the DCVS is detected by the neurobehavioral score and HE staining (the artery wall thickness and internal diameter) (8,9,15). The neurobehavioral score is less specific because the neurobehavioral impairment could occur in a number of brain injuries, including cerebral ischemia and rehaemorrhagia.

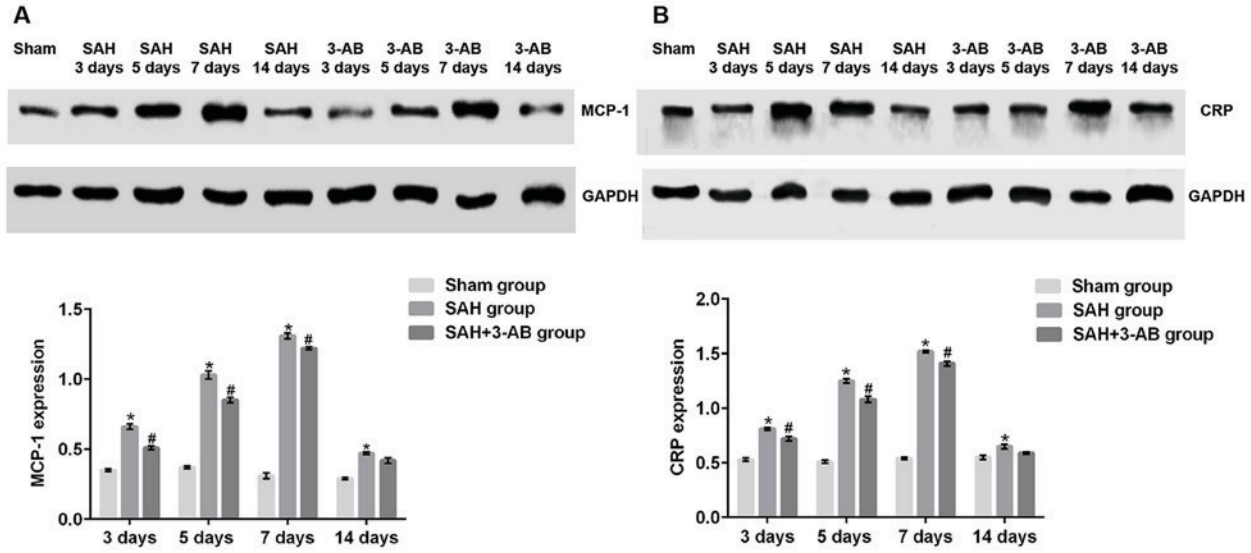

Figure 7. The time course of MCP-1 expression (A) and CRP expression (B) following SAH and the effect of 3-AB on MCP-1 and CRP. The expression of MCP-1 and CRP were tested by western blotting on days 3, 5, 7, 14 post-SAH in the sham group, SAH group and SAH+3-AB group. *P<0.05 vs. the sham group, #P<0.05 vs. the SAH group. SAH, subarachnoid hemorrhage; CRP, C-reactive protein; MCP-1, monocyte chemotactic protein-1; 3-AB, 3-aminobenzamide.

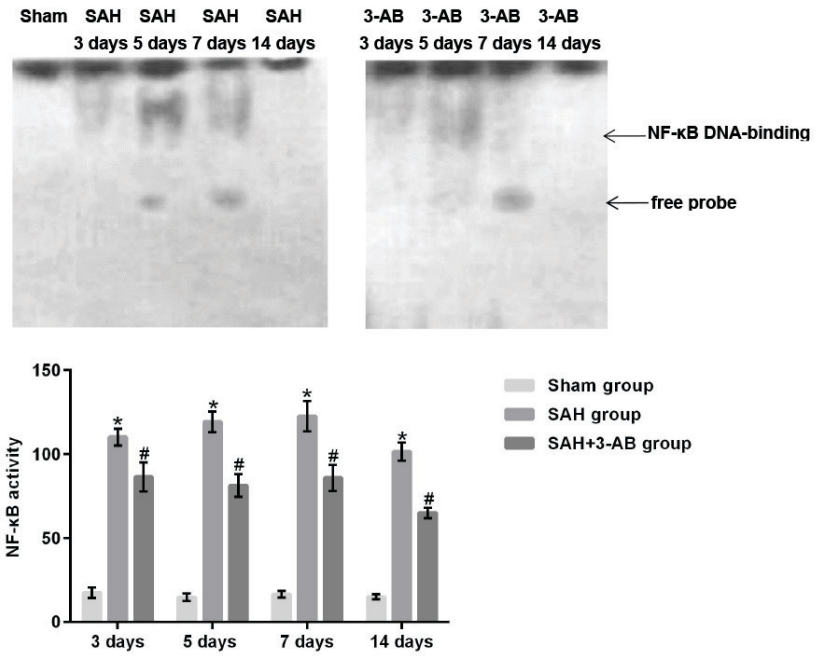

Figure 8. The time course of NF-κB DNA-binding activity following SAH and the effect of 3-AB on NF-κB activity. NF-κB DNA-binding activity was detected by EMSA on days 3, 5, 7, 14 post-SAH in the sham group, SAH group and SAH+3-AB group. *P<0.05 vs. the sham group, #P<0.05 vs. the SAH group. SAH, subarachnoid hemorrhage; NF, nuclear factor.

The increase of wall thickness and the decrease of internal diameter are also the typical characteristics of CVS. By combining the neurobehavioral score and the results of the artery wall thickness and internal diameter, the occurrence of DCVS can be better proved. According to the assessment of neurobehavioral impairment score, the result exhibited a parallel time course to the appearance of DCVS symptoms following SAH. A similar time course occurred in the pathological changes of the basilar artery. All of above results suggested that the rat model of DCVS following SAH was successfully established, thereby providing support for the objectivity of the experiment data.

The formation of DCVS secondary to SAH is a complex pathological process. Previous studies have demonstrated that numerous factors influence DCVS occurrence, including microcirculation, glial-centric mechanisms and endothelial apoptosis (20-22). In previous years, the inflammatory response has been increasingly demonstrated to be involved in the DCVS following SAH (23). In addition to certain upregulated inflammatory factors in DCVS (5,7-9), a series of studies have been performed on the capacity of anti-inflammatory drugs to prevent DCVS. Simvastatin and taurine, for instance, have been demonstrated to alleviate DCVS following SAH in

a rabbit model, which may be associated with the anti-inflammatory effect of statins (24). Although previous studies (7-9) have demonstrated that inflammatory response was involved in the cerebral vasospasm, they mainly focused on cytokines and adhesion molecules, including TNF-α and ICAM-1. In the present study, CRP and MCP-1 were selected to study the inflammatory response in the development of DCVS. The chemokine MCP-1 can direct the migration of specific leukocytes to the sites of inflammation and is therefore involved in certain inflammatory diseases (25,26). Consistent with a previous study (27), MCP-1 in the present study was expressed in a time course parallel to the development of DCVS. Similarly, CRP, an acute phase reactive protein, is known as a highly sensitive inflammatory biomarker in a number of inflammatory diseases including coronary artery disease, ischemic stroke and atherosclerosis (28-30). The CRP expression, for the first time, was detected to be in a parallel time course to the development of DCVS in this study. These results and certain previous findings indicated that inflammatory response is associated with DCVS following SAH. However, the specific mechanism of inflammatory response on DCVS remains unclear.

Accumulating evidence demonstrated that PARP is associated with the pathogenesis of a variety of inflammatory diseases. Adachi *et al* (31) have proved the involvement of PARP activation in the pathogenesis of periodontitis. Mukhopadhyay *et al* (32) have testified that PARP is a key mediator of cisplatin-induced kidney inflammation and injury. Previously, experimental data has demonstrated that PARP participates in the inflammatory pathogenesis of a number of central nervous system disorders including Huntington's disease (33), ischemic stroke (34), traumatic brain injury (35) and neuropathy (36). However, few studies focus on the association between PARP and DCVS, especially over a time course of DCVS development. Therefore, in the present study, for the first time, PARP activity was observed to be in a time course parallel to the development of DCVS following SAH and with the treatment of 3-AB, a PARP inhibitor, DCVS was alleviated. These results indicated that PARP participates in inducing DCVS following SAH. Furthermore, CPR and MCP-1 expressions were reduced under the effect of 3-AB, suggesting that inflammatory response may be mediated by PARP in the development of DCVS. In particular, there have been a number of studies demonstrating positive findings, for example, the inhibition of PARP could prevent neural damage (37), slow down complications of diabetes (38) and exhibit antitumor activity (39) in cell lines or animal models. Following a preliminary mechanism study, the clinical value of 3-AB needs to be further studied via clinical trials. Several PARP inhibitors based on the structure of 3-AB are now being developed clinically (40).

PARP is well-known for two main functions. The first one is detecting and repairing DNA single stand breakage and the second is regulating the inflammatory response through interactions with transcription factors, notably NF-κB (41). NF-κB is a powerful transcription factor that governs the expression of genes encoding cytokines, chemokines, adhesion molecules, growth factors and certain acute phase proteins (7,9,42,43). A previous study has demonstrated that NF-κB in neurons following SAH serves an important role in regulating the expressions of inflammatory genes in the brain (44). Recently, it has been proposed that PARP functioning as a novel coactivator of NF-κB is a common mechanism and a key molecular event involved in the pathogenesis of various inflammatory diseases (45). Furthermore, Castri *et al* (46) have demonstrated that PARP and its cleavage products may modulate the inflammatory response in ischemia models through its function as a coactivator of NF-κB. Chen *et al* (47) have also testified that PARP inhibition attenuates early brain injury in a rat model of SAH through an NF-κB-dependent inflammatory response. In the present study, NF-κB DNA-binding activity exhibited a parallel timeline to PARP activity and was suppressed by 3-AB, suggesting that PARP may regulate inflammatory response through interactions with NF-κB in the development of DCVS. However, the mechanism by which PARP interacts with NF-κB remains controversial and it needs to be further studied.

In conclusion, the results of this study suggest that the inflammatory response mediated by PARP may serve a significant role in the development of DCVS following SAH and inhibition of PARP could attenuate DCVS, providing further rationale for clinical development.

Acknowledgements

Not applicable.

Funding

This study was supported by a grant from the National Natural Science Fund (grant no. 81172598). The sponsor played no role in the design or conduct of this research.

Availability of data and materials

All data generated or analyzed during this study are included in this published article.

Authors' contributions

DY performed EMSA and critically revised the manuscript for important intellectual content. FL was involved in drafting the manuscript and interpreting the data. GY made substantial contributions to conception and design, and took part in performing assessment of neurobehavioral score and measurement of cerebral blood flow. JR performed the western blot experiment and participated in building the model of subarachnoid hemorrhage in rats. WM analyzed and interpreted data. YF performed HE staining, ELISA and was a major contributor in writing the manuscript. All authors read and approved the final manuscript. YY contributed to study design and agreed to be accountable for all aspects of the work in ensuring that questions related to the accuracy of any part of the work are appropriately investigated and resolved.

Ethics approval and consent to participate

Ethical approval was obtained from the Ethical Committee of Xi'an Jiaotong University (no. 0099). All procedures performed in this study involving animals were in accordance with the national standard GB/T16886.2-2011 animal welfare requirements.

Patient consent for publication

Not applicable.

Competing interests

The authors declare they have no competing interests.

References

1. Treggiarivenzi MM, Suter PM and Romand JA: Review of medical prevention of vasospasm after aneurysmal subarachnoid hemorrhage: A problem of neurointensive care. Neurosurgery 48: 249-262, 2001.
2. Woo D and Broderick JP: Spontaneous intracerebral hemorrhage: Epidemiology and clinical presentation. Neurosurg Clin N Am 13: 265-279.v, 2002.
3. Gules I, Satoh M, Clower BR, Nanda A and Zhang JH: Comparison of three rat models of cerebral vasospasm. Am J Physiol Heart Circ Physiol 283: H2551-H2559, 2002.
4. Cecon AD, Figueiredo EG, Bor-seng-shu E, Scaff M and Teixeira MJ: Extremely delayed cerebral vasospasm after subarachnoid hemorrhage. Arq Neuropsiquiatr 66: 554-556, 2008.
5. Wu Q, Zheng R, Wang J, Wang J and Li S: CT perfusion imaging of cerebral microcirculatory changes following subarachnoid hemorrhage in rabbits: Specific role of endothelin-1 receptor antagonist. Brain Res: Sep 20, 2018 (Epub ahead of print).
6. Yatsushige H, Yamaguchi M, Zhou C, Calvert JW and Zhang JH: Role of c-Jun N-terminal kinase in cerebral vasospasm after experimental subarachnoid hemorrhage. Stroke 36: 1538-1543, 2005.
7. Handa Y, Kubota T, Kaneko M, Tsuchida A, Kobayashi H, Kawano H and Kubota T: Expression of intercellular adhesion molecule 1 (ICAM-1) on the cerebral artery following subarachnoid haemorrhage in rats. Acta Neurochir (Wien) 132: 92-97, 1995.
8. Zhang J, Xu X, Zhou D, Li H, You W, Wang Z and Chen G: Possible role of Raf-1 kinase in the development of cerebral vasospasm and early brain injury after experimental subarachnoid hemorrhage in rats. Mol Neurobiol 52: 1527-1539, 2015.
9. Zhou ML, Shi JX, Hang CH, Cheng HL, Qi XP, Mao L, Chen KF and Yin HX: Potential contribution of nuclear factor-kappaB to cerebral vasospasm after experimental subarachnoid hemorrhage in rabbits. J Cereb Blood Flow Metab 27: 1583-1592, 2007.
10. Pacher L and Szabó C: Role of Poly(ADP-Ribose) polymerase-1 activation in the pathogenesis of diabetic complications: Endothelial dysfunction, as a common underlying theme. Antioxid Redox Signal 7: 1568-1580, 2005.
11. Pacher P, Mabley JG, Soriano FG, Liaudet L and Szabó C: Activation of poly(ADP-ribose) polymerase contributes to the endothelial dysfunction associated with hypertension and aging. Int J Mol Med 9: 659-664, 2002.
12. Hassa PO, Buerki C, Lombardi C, Imhof R and Hottiger MO: Transcriptional coactivation of nuclear factor-kappaB-dependent gene expression by p300 is regulated by Poly(ADP)-ribose polymerase-1. J Biol Chem 278: 45145-45153, 2003.
13. Saravanan S, Islam VI, Babu NP, Pandikumar P, Thirugnanasambantham K, Chellappandian M, Raj CS, Paulraj MG and Ignacimuthu S: Swertiamarin attenuates inflammation mediators via modulating NF-κB/I κB and JAK2/STAT3 transcription factors in adjuvant induced arthritis. Eur J Pharm Sci 56: 70-86, 2014.
14. Kaoutzanis M, Yokota M, Sibilia R and Peterson JW: Neurologic evaluation in a canine model of single and double subarachnoid hemorrhage. J Neurosci Methods 50: 301-307, 1993.
15. Xiong Y, Wang XM, Zhong M, Li ZQ, Wang Z, Tian ZF, Zheng K and Tan XX: Alterations of caveolin-1 expression in a mouse model of delayed cerebral vasospasm following subarachnoid hemorrhage. Exp Ther Med 12: 1993-2002, 2016.
16. Shao A, Guo S, Tu S, Ammar AB, Tang J, Hong Y, Wu H and Zhang J: Astragaloside IV alleviates early brain injury following experimental subarachnoid hemorrhage in rats. Int J Med Sci 11: 1073-1081, 2014.
17. Grasso G: An overview of new pharmacological treatments for cerebrovascular dysfunction after experimental subarachnoid hemorrhage. Brain Res Brain Res Rev 44: 49-63, 2004.
18. Specogna AV: Subarachnoid hemorrhage diagnosis. JAMA 311: 201, 2014.
19. Sousa FG, Matuo R, Soares DG, Escargueil AE, Henriques JA, Larsen AK and Saffi J: PARPs and the DNA damage response. Carcinogenesis 33: 1433-1440, 2012.
20. Chai WN, Sun XC, Lv FJ, Wan B and Jiang L: Clinical study of changes of cerebral microcirculation in cerebral vasospasm after SAH. Acta Neurochir Suppl 110: 225-228, 2011.
21. Mutch WA: New concepts regarding cerebral vasospasm: Glial-centric mechanisms. Can J Anaesth 57: 479-489, 2010.
22. Yan JH, Yang XM, Chen CH, Hu Q, Zhao J, Shi XZ, Luan LJ, Yang L, Qin LH and Zhou CM: Pifithrin-alpha reduces cerebral vasospasm by attenuating apoptosis of endothelial cells in a subarachnoid haemorrhage model of rat. Chin Med J (Engl) 121: 414-419, 2008.
23. Pluta RM: Introduction to problems of postsubarachnoid hemorrhage delayed cerebral vasospasm. Animal Models of Acute Neurological Injuries II, pp459-464, 2012.
24. Lin C, Zhao Y, Wan G, Zhu A and Wang H: Effects of simvastatin and taurine on delayed cerebral vasospasm following subarachnoid hemorrhage in rabbits. Exp Ther Med 11: 1355-1360, 2016.
25. Zaheer A, Sahu SK, Wu Y, Zaheer A, Haas J, Lee K and Yang B: Diminished cytokine and chemokine expression in the central nervous system of GMF-deficient mice with experimental autoimmune encephalomyelitis. Brain Res 1144: 239-247, 2007.
26. Thompson WL, Karpus WJ and Van Eldik LJ: MCP-1-deficient mice show reduced neuroinflammatory responses and increased peripheral inflammatory responses to peripheral endotoxin insult. J Neuroinflammation 5: 35, 2008.
27. Lu H, Shi JX, Chen HL, Hang CH, Wang HD and Yin HX: Expression of monocyte chemoattractant protein-1 in the cerebral artery after experimental subarachnoid hemorrhage. Brain Res 1262: 73-80, 2009.
28. Buckley DI, Fu R, Freeman M, Rogers K and Helfand M: C-reactive protein as a risk factor for coronary heart disease: A systematic review and meta-analyses for the U.S. preventive services task force. Ann Intern Med 151: 483-495, 2009.
29. Elkind MS, Luna JM, Moon YP, Liu KM, Spitalnik SL, Paik MC and Sacco RL: High-sensitivity C-reactive protein predicts mortality but not stroke the northern manhattan study. Neurology 73: 1300-1307, 2009.
30. Nordestgaard BG and Zacho J: Lipids, atherosclerosis and CVD risk: Is CRP an innocent bystander? Nutr Metab Cardiovasc Dis 19: 521-524, 2009.
31. Adachi K, Miyajima SI, Nakamura N, Miyabe M, Kobayashi Y, Nishikawa T, Suzuki Y, Kikuchi T, Kobayashi S, Saiki T, *et al*: Role of Poly(ADP-ribose) polymerase activation in the pathogenesis of periodontitis in diabetes. J Clin Periodontol 44: 971-980, 2017.
32. Mukhopadhyay P, Horváth B, Kechrid M, Tanchian G, Rajesh M, Naura AS, Boulares AH and Pacher P: Poly(ADP-ribose) polymerase-1 is a key mediator of cisplatin-induced kidney inflammation and injury. Free Radic Biol Med 51: 1774-1788, 2011.
33. Cardinale A, Paldino E, Giampà C, Bernardi G and Fusco FR: PARP-1 inhibition is neuroprotective in the R6/2 mouse model of Huntington's disease. PLoS One 10: e134482, 2015.
34. Sun M, Zhao Y, Gu Y and Xu C: Anti-inflammatory mechanism of taurine against ischemic stroke is related to down-regulation of PARP and NF-κB. Amino Acids 42: 1735-1747, 2012.
35. Besson VC, Zsengellér Z, Plotkine M, Szabó C and Marchand-Verrecchia C: Beneficial effects of PJ34 and INO-1001, two novel water-soluble poly(ADP-ribose) polymerase inhibitors, on the consequences of traumatic brain injury in rat. Brain Res 1041: 149-156, 2005.
36. Komirishetty P, Areti A, Gogoi R, Sistla R and Kumar A: Combination strategy of PARP inhibitor with antioxidant prevent bioenergetic deficits and inflammatory changes in CCI-induced neuropathy. Neuropharmacology 113: 137-147, 2017.
37. Song ZF, Ji XP, Li XX, Wang SJ, Wang SH and Zhang Y: Inhibition of the activity of poly (ADP-ribose) polymerase reduces heart ischaemia/reperfusion injury via suppressing JNK-mediated AIF translocation. J Cell Mol Med 12: 1220-1228, 2008.
38. Pandya KG, Patel MR and Lau-Cam CA: Comparative study of the binding characteristics to and inhibitory potencies towards PARP and in vivo antidiabetogenic potencies of taurine, 3-aminobenzamide and nicotinamide. J Biomed Sci 17 (Suppl 1): S16, 2010.
39. Finn RS, Lau A, Kalous O, Conklin D, Dering J, Knights C, O Shaughnessy A, Cranston A, Riches L and Carmichael J: Pre-clinical activity of the PARP inhibitor AZD2281 in human breast cancer cell lines and in combination with DNA damaging agents. Cancer Res 69: 1038, 2009.

40. Sandhu SK, Yap TA and de Bono JS: Poly(ADP-ribose) polymerase inhibitors in cancer treatment: A clinical perspective. Eur J Cancer 46: 9-20, 2010.
41. d'Avila JC, Lam TI, Deborah B, Shi J, Won SJ, Kauppinen TM, Massa S, Liu J and Swanson RA: Microglial activation induced by brain trauma is suppressed by post-injury treatment with a PARP inhibitor. J Neuroinflamm 9: 31, 2012.
42. Nakajima H, Nagaso HN, Ishikawa M, Hiranuma T and Hoshiko S: Critical role of the automodification of poly(ADP-ribose) polymerase-1 in nuclear factor-kappaB-dependent gene expression in primary cultured mouse glial cells. J Biol Chem 279: 42774-42786, 2004.
43. Chen F, Castranova V, Shi X and Demers LM: New insights into the role of nuclear factor-kappaB, a ubiquitous transcription factor in the initiation of diseases. Clin Chem 45: 7-17, 1999.
44. You WC, Wang CX, Pan YX, Zhang X, Zhou XM, Zhang XS, Shi JX and Zhou ML: Activation of nuclear factor-κB in the brain after experimental subarachnoid hemorrhage and its potential role in delayed brain injury. PLoS One 8: e60290, 2013.
45. Hassa PO and Hottiger MO: The functional role of poly(ADP-ribose)polymerase 1 as novel coactivator of NF-kappaB in inflammatory disorders. Cell Mol Life Sci 59: 1534-1553, 2002.
46. Castri P, Lee YJ, Ponzio T, Maric D, Spatz M, Bembry J and Hallenbeck J: Poly(ADP-ribose) polymerase-1 and its cleavage products differentially modulate cellular protection through NF-kappaB-dependent signaling. Biochim Biophys Acta 1843: 640-651, 2014.
47. Chen T, Wang W, Li JR, Xu HZ, Peng YC, Fan LF, Yan F, Gu C, Wang L and Chen G: PARP inhibition attenuates early brain injury through NF-κB/MMP-9 pathway in a rat model of subarachnoid hemorrhage. Brain Res 1644: 32-38, 2016.